Chapter 3

Quantitative Dixon and qualitative T1 MRI sequences to relate muscle atrophy and fatty degeneration with range of motion and muscle force in brachial plexus injury

B.J. Duijnisveld [1], J.F. Henseler [1], M. Reijnierse [2], M. Fiocco [3, 4], H.E. Kan [5], R.G.H.H. Nelissen [1]

1. Department of Orthopaedics, Leiden University Medical Center
2. Department of Radiology, Leiden University Medical Center
3. Department of Medical Statistiscs and Bioinformatics, Leiden University Medical Center
4. Mathematica Institute, Leiden University
5. C.J. Gorter Center for High Field MRI, department of Radiology, Leiden University Medical Center

Submitted

ABSTRACT

Background: Assessment of muscle atrophy and fatty degeneration in brachial plexus injury (BPI) could yield valuable insight into pathophysiology and could be used to predict clinical outcome. The objective of this study was to quantify and relate fat percentage and cross-sectional area (CSA) of the biceps to range of motion and muscle force of traumatic brachial plexus injury (BPI) patients.

Methods: T1- weighted TSE sequence and three-point Dixon images of the affected and non-affected biceps brachii were acquired on a 3 Tesla magnetic resonance scanner to determine the Goutallier score, fat percentage, total and contractile CSA of 20 adult BPI patients. Regions of interest were drawn by two independent investigators to determine the inter-observer reliability. Paired Students' t-test and multivariate analysis were used to relate fat percentage, total and contractile CSA to active flexion and biceps muscle force.

Results: The mean fat percentage 12 ± 5.1% of affected biceps was higher than 6 ± 1.0% of the non-affected biceps ($p < 0.001$). The mean contractile CSA 8.1 ± 5.1 cm^2 of the affected biceps was lower than 19.4 ± 4.9 cm^2 of the non-affected biceps ($p < 0.001$). The inter-observer reliability was excellent (ICC 0.82 to 0.96). The Goutallier score was strongly associated with fat percentage (Spearman's rho 0.87, $p < 0.001$), however it gave an overestimation in those classified with a high grade Goutallier. The contractile CSA contributed most to the reduction in active flexion and muscle force.

Conclusion: Quantitative measurement of fat percentage, total and contractile CSA using three-point Dixon sequences provides an excellent reliability and relates with active flexion and muscle force in BPI.

INTRODUCTION

Brachial plexus injury (BPI) results in severe nerve damage affecting the upper extremity. Despite partial natural recovery, nerve and/or secondary surgery, both traumatic BPI patients and neonatal brachial plexus palsy patients do not regain normal upper extremity function and are impaired in muscle force and range of motion of the shoulder, elbow, wrist and/or hand [1-7]. Long-term denervation results in muscle degeneration including muscle atrophy, fatty degeneration and interstitial fibrosis in the muscle. Quantitative tools which assess the decrease in the amount of muscle tissue could improve insight in the extent of muscle degeneration and could facilitate a better treatment strategy. The current literature on muscle degeneration in the upper extremity of BPI focuses on total muscle cross sectional area (CSA) and on a qualitative assessment of muscle fatty degeneration using the Goutallier score on T1 weighted Turbo Spin Echo (TSE) magnetic resonance (MR) images as well as at computed tomography (CT) scans [4, 7-13]. The current literature has limitations as the inter-observer reliability of the Goutallier score is moderate even in experienced hands [14, 15]. Furthermore, a qualitative assessment of fatty degeneration is less sensitive in detecting small differences compared to a quantitative assessment [16-18]. Finally, an overall qualitative muscle score (i.e. Goutallier score) and assessments of total muscle CSA measure both fatty degeneration as well as contractile muscle tissue, whereas only the latter is the true functional part of the muscle [4, 7-13].

The three-point Dixon sequence can be applied to quantify intramuscular fat (i.e. indirect contractile muscle tissue). This sequence uses a chemical shift based approach which relies on the difference in resonance frequency between water and fat. Previously, the Dixon sequence has been used extensively to measure intramuscular fat in different conditions, including rotator cuff tears [19, 20], lean and obese children [21], diabetes [22, 23] and the muscular dystrophies [17, 18, 24-30]. However, the extent of muscle fatty degeneration as an indirect measure and the amount of contractile tissue in BPI is currently unknown.

The first objective of this study was to quantify intramuscular fat, the total and contractile CSA in BPI patients and to assess the inter-observer reliability and the variability using three-point Dixon MRI. The second objective was to correlate the qualitatively assessed intramuscular fat with the Goutallier score on a T1 weighted TSE sequence with the quantitatively obtained value. The final objective was to assess whether intramuscular fat, the total and contractile CSA were associated with elbow range of motion and muscle force in severely affected BPI patients.

METHODS

Patients

An observational study was performed including 20 adult BPI patients recruited from the peripheral nerve injury unit of the Leiden University Medical Center. Inclusion criteria were an age > 18 years old and a traumatic BPI. To create a uniform group of patients who are at the end stage of neural regeneration, all patients had to be minimum two years after trauma and/or nerve surgery for the biceps muscle. Patients were excluded if they had a fracture of the humeral bone, bilateral brachial plexus lesion, secondary surgery around the shoulder or elbow, or contra-indications for MRI. The medical ethical review board of the Leiden University Medical Center approved the protocol of this study and all patients signed informed consent. This study was registered in the Netherlands Trial Register, number NTR2524.

MRI

MR imaging was performed on a 3 Tesla MR machine (Philips Achieva, Philips Medical Systems, Best, the Netherlands) in supine position, with the arm as much in the center of the magnet bore as possible and the patient's arms placed alongside of the body with the thumbs directed upwards. Both arms were imaged separately. A 14-cm two-element receive coil was used for signal reception. The receive coil elements were positioned on the anterior and posterior side in the middle of the upper arm using the humeral head and olecranon as palpable bony reference. The scan protocol consisted of axial T1-weighted TSE sequence (16 slices of 7.5 mm thickness, 0.75 mm gap, repetition time (TR) 600 ms, echo time (TE) 16 ms, field of view (FOV) 180 x 180 mm, voxel size 0.6x0.6 mm^2, TSE factor 5, acquisition time 5:20 minutes) and a 3-point gradient echo Dixon sequence (16 slices of 7.5 mm thickness, 0.75 mm gap, TR 400 ms, first TE 4.41 ms, echo spacing 0.76 ms, flip angle 8°, FOV 180x180 mm, (voxel size 0.9x0.9 mm^2), acquisition time 6:30 minutes) of the affected and non-affected upper arm. The T1 and Dixon sequences were planned using a survey scan, around the distal 2/3 of the humeral bone using the humeral head and epicondyles of the distal humeral bone as bony landmark. Representative examples of T1, Dixon fat and Dixon water images of the non-affected and affected arm are shown in figure 1.

Data analysis

The three-point Dixon images were reconstructed with multipeak correction as described before, with frequencies f_p = [94, -318, -420] Hz and amplitudes A_p = [0.08, 0.15, 0.78], to account for the multiple peaks of the fat spectrum [28]. No corrections were made for partial saturation due to T1, T2 or T2* relaxation. Regions of interest

(ROIs) were drawn manually on every slice by two independent investigators (B.J.D. and J.F.H.), blinded for patient details using the Medical Image Processing, Analysis and Visualization software package (http://mipav.cit.nih.gov) on T1-weighted images in the biceps and triceps brachii of the affected and non-affected arm. Five consecutive slices with the largest cross sectional area of the biceps and triceps brachii were used to calculate the mean fat percentage, the total CSA (i.e. the CSA including muscle tissue and intramuscular fat tissue), and the contractile CSA which was calculated from the mean fat percentage and the total CSA (contractile CSA = total CSA (100 - mean fat percentage) / 100). The mean fat percentage per muscle was computed using the co-registered contours from the T1 weighted images on the Dixon images and calculated by averaging all pixels assigned to that muscle. Next, the mean fat percentage was calculated by: signal intensity on fat image / (signal intensity on fat image + signal intensity at water image). The Goutallier grading was scored by two experienced musculoskeletal radiologists (CSPR and MR) in consensus: 0 'no fat', 1 'some fatty streaks', 2 'less fat than muscle', 3 'as much fat as muscle' and 4 'more fat than muscle'. Furthermore, the affected biceps and triceps brachii were scored for the presence of atrophy compared to the non-affected biceps and triceps brachii of the contra lateral arm.

Clinical parameters

The age, gender, affected side, severity of the lesion according to Narakas and type of nerve and/or secondary surgery was recorded [31]. The passive and active elbow range of motion (flexion, extension, supination and pronation) was measured using a hand held goniometer. Muscle force was measured (semi) quantitatively of both elbow flexion and elbow extension using the medical research council (MRC) scale and a hand-held dynamometer (MicroFET2, Biometrics, Almere, the Netherlands) in a standardized arm positions (90° flexion and 90° supination). Muscle quality was determined by calculating the specific muscle force i.e. muscle force in Newton per cm^2 of contractile CSA. The self assessment questionnaires disability of the arm, shoulder and hand (DASH), the short form-36 (SF-36) and visual analogue score (VAS) for pain (0-10) were used to assess the quality of life of the BPI patients.

Statistical analysis

The paired Student's t-test was used to study differences in fat percentage, total CSA, contractile CSA and specific muscle force between the affected and the non-affected biceps and triceps brachii. The intraclass correlation coefficient (ICC) of fat percentage, total and contractile CSA was calculated to determine the reliability between two independent observers and potential variability between 5 consecutive MRI slices using the 2-way random model with absolute agreement [32].

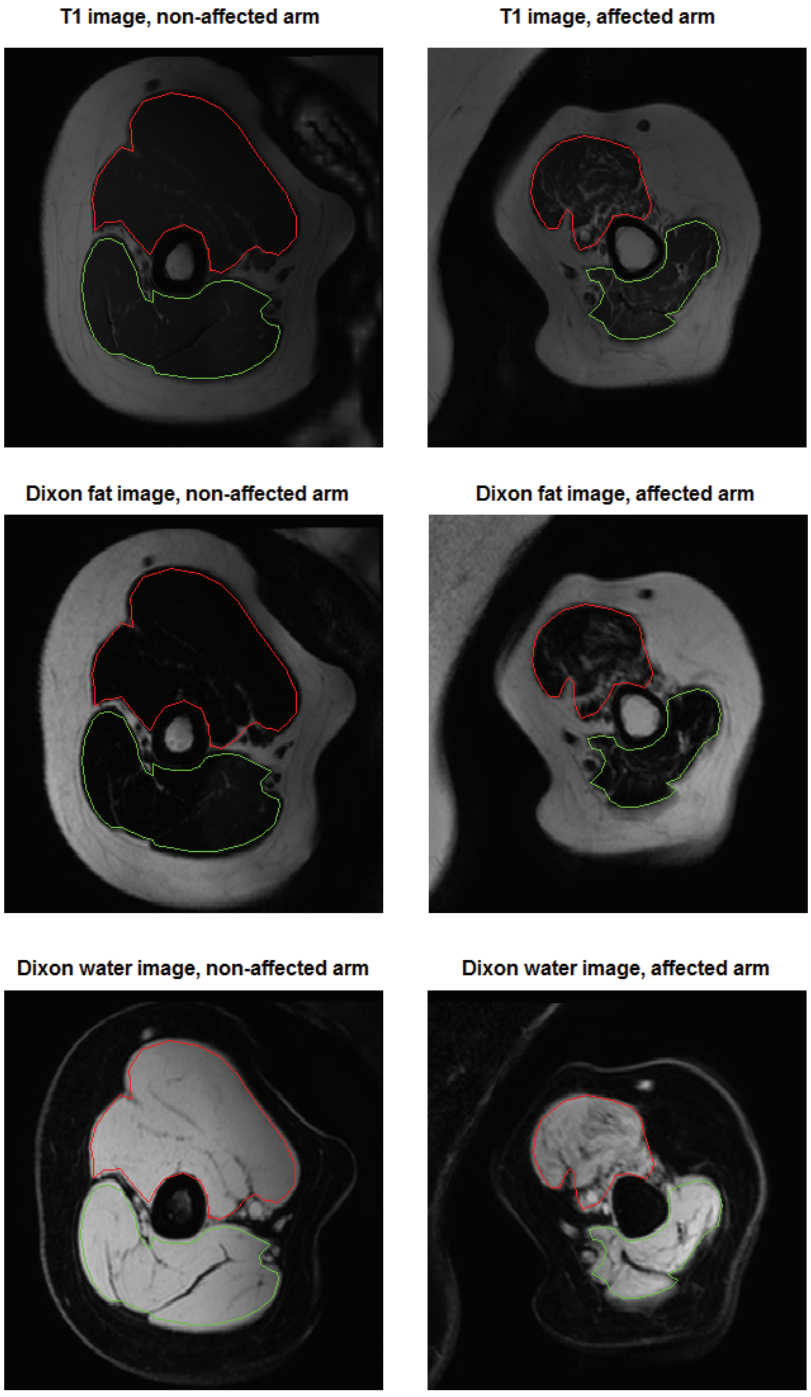

Figure 1: Example of T1, Dixon fat and Dixon water images of the non-affected and affected arm. Regions of interest are drawn in red for the biceps and green for the triceps brachii.

For interpretation, the criteria formulated by Cicchetti and Sparrow were used: 0.00 to 0.39, poor; 0.40 to 0.59, fair; 0.60 to 0.74, good; or 0.75 to 1.00, excellent [33]. The Spearman's rho correlation coefficient was used to investigate the presence of correlation between the percentages of fat using Dixon with the Goutallier score of the T1w images. Univariate linear regression analysis was employed to study the association between fat percentage, total and contractile CSA with range of motion and muscle force in Newton. Logistic regression analysis was used to associate fat percentage, total and contractile CSA to muscle force in MRC 0 to 3 versus MRC 4 and 5. In the multivariate analysis, age and elapsed time since the trauma were used. For statistical analysis a SPSS software package was used (version 23.0, IBM Inc., Armonk, New York, USA). All analyses were two tailed and *p*-values < 0.05 were considered significant.

RESULTS

Patients

The patient characteristics are summarized in table I. In one patient, the non-affected arm could not be scanned due to claustrophobia of the patient after scanning the affected arm. The mean fat percentage was 12 ± 5.1 % in the affected biceps brachii which was significantly higher than 6 ± 1.0 % in the non-affected biceps brachii ($p < 0.001$) as shown in figure 2. The mean fat percentage was 10 ± 4.3 % in the affected triceps brachii, compared to 6 ± 1.6 % of the non-affected triceps brachii ($p = 0.001$). The mean total CSA of the affected biceps brachii was 9.0 ± 5.3 cm^2 which was lower than a mean of 20.7 ± 5.2 cm^2 of the non-affected biceps brachii ($p = 0.001$). The mean contractile CSA was lower in the affected biceps brachii 8.1 ± 5.1 cm^2, compared to a mean of 19.4 ± 4.9 cm^2 in the non-affected biceps brachii ($p < 0.001$). The total and contractile CSA were also lower in the affected triceps brachii compared to the non-affected triceps brachii as shown in table II.

Reliability

The interobserver reliability was excellent for fat percentage, total CSA and contractile CSA in both the biceps and the triceps brachii (table III). To measure the homogeneity between the MRI slices, the ICC of 5 consecutive MRI slices was calculated. The ICC was excellent for fat percentage, total and contractile CSA of the biceps brachii and the triceps brachii (table III).

Table I: Patient characteristics

	N = 20
Sex * (male)	17
Age † (years)	37 ± 11.1
Body mass index† (kg/m^2)	25 ± 3.8
Dominancy before trauma * (right / left / both)	16 / 3 / 1
Brachial plexus injury	
Age at trauma † (years)	31 ± 10.8
Side * (right / left)	10 / 10
Narakas type* (C5-C6 / C5-C7 / C5-C8 / C5-T1)	5 / 1 / 3 / 11
Primary treatment	
Conservative / neurolysis / nerve transplantation *	4 / 1 / 15
Age at neurosurgery † (years)	31 ± 11.3
Type of nerve transplantation *	
Anterior division superior trunk	6
Posterior division superior trunk	3
Medial trunk	1
Suprascapular nerve	2
Musculus cuteneus nerve	8
SF36 questionnaire †#	72 ± 18.1
DASH questionnaire †‡	23 ± 17.6
Employed *#	16
Playing sport / instrument*#	9
VAS for pain †#	3.5 ± 3.06

*The values are given as the number of patients. † Values are given as mean with standard deviation #data was obtained from 19 patients, ‡data was obtained from 18 patients. SF36: Short-Form 36. DASH: Disability of the arm, shoulder and hand. VAS: Visual analogue scale with range from 0 ´no pain´ to 10 ´maximum pain´.

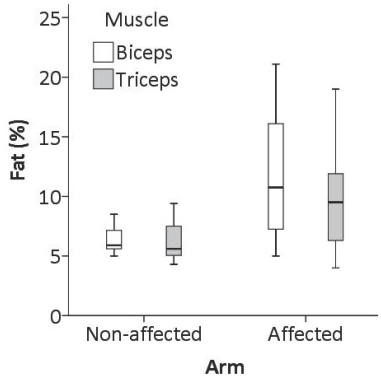

Figure 2: Fat percentage of the affected en non-affected biceps and triceps

Table II: Results of fat percentage, total and contractile CSA in the affected and non-affected biceps and triceps brachii

	Affected arm	Non-affected arm	Mean difference (95 % CI)	*p* - value
Fat (%)				
Biceps brachii	12 ± 5.1	6 ± 1.0	-5 (-3 to -7)	< 0.001
Triceps brachii	10 ± 4.3	6 ± 1.6	-3 (-2 to -5)	0.001
Total CSA * (cm^2)				
Biceps brachii	9.0 ± 5.3	20.7 ± 5.2	-11.5 (-15.0 to -7.9)	< 0.001
Triceps brachii	10.3 ± 6.6)	20.2 ± 4.8	-9.5 (-12.7 to -6.4)	< 0.001
Contractile CSA # (cm^2)				
Biceps brachii	8.1 ±5.1	19.4 ± 4.9	-11.1 (-14.5 to -7.7)	< 0.001
Triceps brachii	9.4 ±6.3	18.9 ± 4.5	-9.1 (-12.1 to -6.2)	< 0.001

*The CSA including muscle tissue and intramuscular fat tissue, #contractile CSA = total CSA (100 - mean fat percentage) / 100, CI: confidence interval, CSA: cross sectional area.

Table III: Intraclass correlation coefficients of 2 independent observers and 5 consecutive MRI slices

	2 independent observers			5 consecutive MRI slices		
	ICC	95 % CI	p-value	ICC	95 % CI	p-value
Muscle fat (%)						
Biceps brachii	0.88	0.73 – 0.94	< 0.001	0.94	0.91 – 0.96	< 0.001
Triceps brachii	0.82	0.65 – 0.89	< 0.001	0.92	0.87 – 0.95	< 0.001
Total CSA * (cm^2)						
Biceps brachii	0.95	0.43 – 0.99	< 0.001	0.99	0.98 – 0.99	< 0.001
Triceps brachii	0.96	0.56 – 0.99	< 0.001	0.95	0.92 – 0.97	< 0.001
Contractile CSA # (cm^2)						
Biceps brachii	0.88	0.36 – 0.96	< 0.001	0.99	0.99 – 1.00	< 0.001
Triceps brachii	0.89	0.45 – 0.96	< 0.001	0.95	0.92 – 0.97	< 0.001

*The CSA including muscle tissue and intramuscular fat tissue, #contractile CSA = total CSA (100 - mean fat percentage) / 100. MRI: magnetic resonance imaging, ICC: interclass correlation coefficient, CI: confidence interval, CSA: cross sectional area.

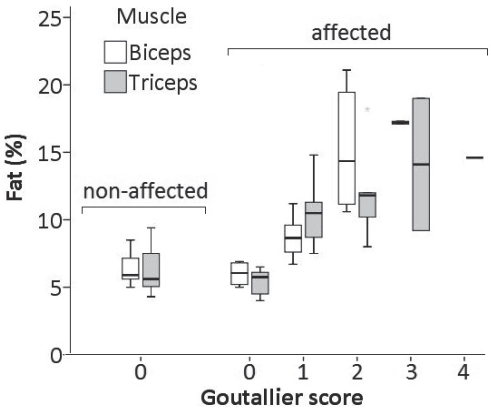

Figure 3: Association of quantitative fat percentage on Dixon with qualitative Goutallier score on T1 of the affected and non-affected biceps and triceps

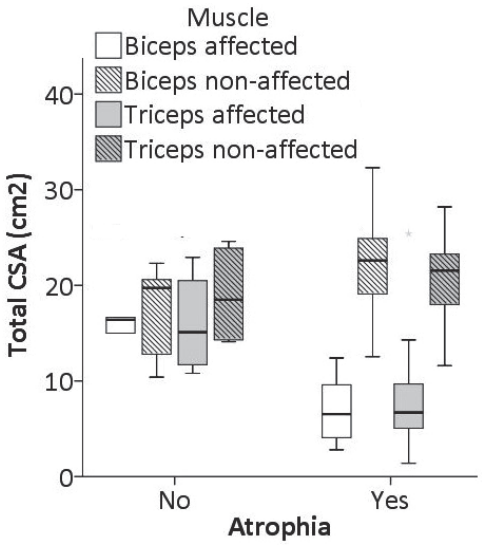

Figure 4: Association of total cross sectional area with atrophy of the affected and non-affected biceps and triceps

Qualitative versus quantitative fat scores

The quantitative fat percentage was strongly associated with the qualitative Goutallier score with a Spearman's rho correlation coefficient of 0.87 for the biceps ($p < 0.001$) and 0.78 for the triceps ($p < 0.001$), as depicted in figure 3. However, the Goutallier score overestimates the fat percentage as patients graded with score 3 or 4 (i.e. fat percentage of 50% or higher) had a three-point Dixon fat percentage range from 9 to 19%. The qualitative score of atrophy was compared to the quantitative score of total CSA, as shown in figure 4. In the patients where the mean total CSA of the biceps brachii was visually scored as 'not atrophic', there was indeed no significant difference between the affected and the non-affected arm (mean difference -1.6 cm^2, 95% CI 4,8 to 1.6, $p = 0.23$). Also the mean total CSA of the triceps brachii which were scored as 'not atrophic', was not significantly different between the affected and the non-affected arm (mean difference -2.9 cm^2, 95% CI -7.7 to 2.0, $p = 0.18$). The mean total CSA of biceps brachii which were scored 'atrophic' was significantly smaller in the affected compared to the non-affected biceps (mean difference -15.0 cm^2, 95% CI -17.7 to -12.3, $p < 0.001$). The same results were observed for the triceps brachii (mean difference -11.9 cm^2, 95% CI -15.1 to -8.7, $p < 0.001$).

Relation to clinical outcome

The association of fat percentage, total and contractile CSA of the affected and non-affected biceps and triceps brachii with muscle force in MRC is shown in figure 5. Clinical results of passive and active range of motion and muscle force are shown in table IV. The specific muscle force was lower in the affected biceps brachii (mean 10 ± 5.4 N/cm^2) compared to the non-affected biceps (mean 16 ± 4.8 N/cm^2) ($p = 0.002$), while this failed to reach significance in the triceps brachii (mean 12 ± 4.9 N/cm^2 in the affected versus 14 ± 3.6 N/cm^2 in the unaffected arm ($p = 0.078$). Univariate and multivariate regression analyses are described in tables V to VII. Multivariate regression analysis showed that contractile CSA of the biceps brachii was most significantly related to several clinical outcome parameters including elbow flexion (7.1°, 95% CI 2.8 to 11.5, $p = 0.003$), supination (5.5°, 95% CI 0.6 to 10.4, $p = 0.030$), muscle force in MRC (odds ratio 2.6, 95% CI 1.1 to 6.1) and muscle force in Newton (13.0N, 95% CI 8.9 to 17.1).

Table IV: Clinical results

	Muscle force of the affected biceps brachii						Non- affected
	MRC 0 N = 3	MRC 1 N = 2	MRC 2 N = 1	MRC 3 N = 2	MRC 4 N = 10	MRC 5 N = 2	Biceps brachii N = 20
Active flexion † (°)	-	-	60	83 ± 10.6	133 ± 15.9	145 ± 7.1	140 (150 – 150)
Active extension † (°)	-	-	-20	-15 ± 7.1	-9 ± 9.7	-5 ± 7.1	0 (0 – 0)
Active pronation † (°)	-	45 ± 64	30	45 ± 63.6	69 ± 33.8	80 ± 14.1	90 (90 – 90)
Active supination † (°)	-	-	-30	-40 ± 56.6	25 ± 54.9	90 ± 0.0	90 (90 – 90)
Passive flexion † (°)	118 ± 18.9	145 ± 7.1	140	133 ± 3.5	143 ± 10.3	150 ± 0.0	143 (150 – 150)
Passive extension † (°)	-11 ± 7.6	-	-20	-15 ± 7.1	-7 ± 8.5	-5 ± 7.1	0 (0 – 0)
Passive pronation † (°)	90 ± 0.0	90 ± 0.0	90	90 ± 0.0	82 ± 16.2	90 ± 0.0	90 (90 – 90)
Passive supination † (°)	50 ± 34.6	15 ± 21	-30	0 ± 0.0	5 ± 37.3	90 ± 0.0	90 (90 – 90)
Force triceps ‡ (MRC)	0 (0 – 0)	2 (0 – 4)	0	0 (0 – 0)	4 (3 – 4)	5 (5 – 5)	5 (5 – 5)
Force biceps † (Newton)	-	-	-	-	90 ± 61.4	193 ± 67.2	306 ± 55.2
Force triceps † (Newton)	-	38 ± 54	-	-	125 ± 93.6	214 ± 48.8	248 ± 63.6
Upper arm circumference † (cm)	23 ± 2.6	21 ± 3.2	26	29 ± 1.4	24 ± 2.5	26 ± 1.4	29 ±2.8

†The values are given as mean with standard deviation. ‡The values are given as median with inter quartile range. MRC: medical research council.

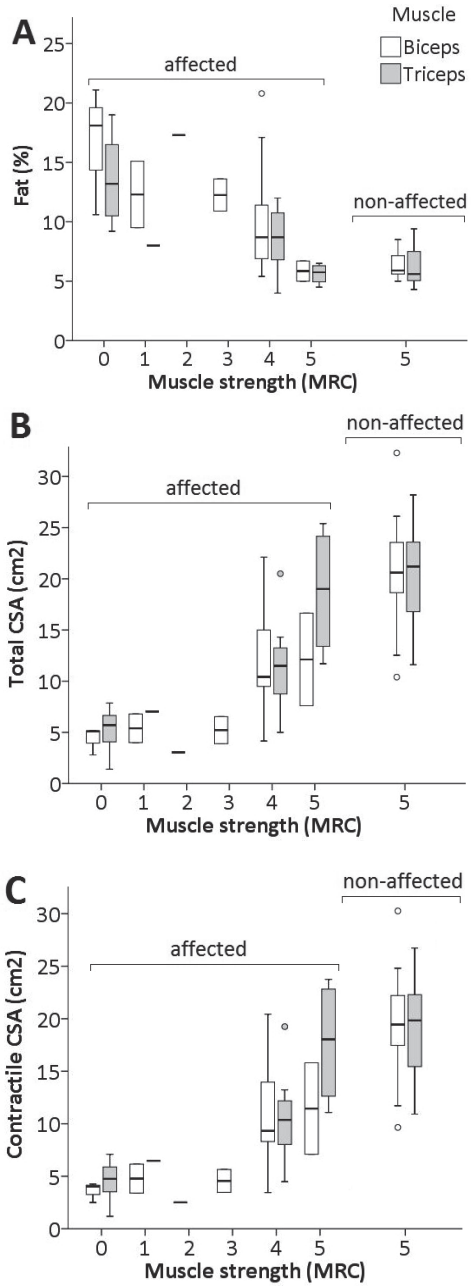

Figure 5: Association of fat percentage (A), total CSA (B) and contractile CSA (C) with muscle force of the affected and the non-affected biceps and triceps

Table V: Linear regression for active range of motion

	Regression coefficient	95% CI	*p* - value
Active flexion univariate models for the affected biceps brachii			
Fat percentage	-6.0	-10.8 to -1.2	0.017
Total CSA *	7.0	2.8 to 11.2	0.003
Contractile CSA #	7.3	2.9 to 11.7	0.003
Active flexion multivariate models for the affected biceps brachii			
Fat percentage	-5.9	-10.9 to -0.8	0.025
Total CSA *	6.8	2.6 to 11.0	0.004
Contractile CSA #	7.1	2.8 to 11.5	0.003
Active extension univariate models for the affected triceps brachii			
Fat percentage	-0.9	-1.8 to 0.05	0.061
Total CSA *	0.6	-0.03 to 1.2	0.062
Contractile CSA #	0.6	-0.02 to 1.2	0.058
Active extension multivariate models for the affected triceps brachii			
Fat percentage	-1.0	-1.8 to 0.1	0.029
Total CSA *	-0.4	-0.2 to 1.0	0.159
Contractile CSA #	0.5	-0.2 to 1.1	0.150
Active supination univariate models for the affected biceps brachii			
Fat percentage	-3.2	-8.0 to 1.7	0.186
Total CSA *	4.8	0.5 to 9.1	0.031
Contractile CSA #	5.0	0.5 to 9.4	0.032
Active supination multivariate models for the affected biceps brachii			
Fat percentage	-3.8	-9.2 to 1.7	0.164
Total CSA *	5.2	0.6 to 9.9	0.030
Contractile CSA #	5.5	0.6 to 10.4	0.030

*The CSA including muscle tissue and intramuscular fat tissue, #contractile CSA = total CSA (100 - mean fat percentage) / 100. Univariate linear regression models evaluated the associate fat percentage, total CSA or contractile CSA of the affected biceps or triceps brachii to active range of motion. The multivariate models were used to correct for age and time after trauma. CI: confidence interval, CSA: cross sectional area.

Table VI: Logistic regression for muscle force in MRC

	Odds ratio	95% CI	*p* - value
Univariate models for the affected biceps brachii			
Fat percentage	-0.17	-0.31 to -0.04	0.012
Total CSA *	0.16	0.02 to 0.29	0.024
Contractile CSA #	0.17	0.03 to 0.32	0.021
Multivariate models for the affected biceps brachii			
Fat percentage	0.7	0.55 to 0.99	0.045
Total CSA *	2.4	1.1 to 5.6	0.034
Contractile CSA #	2.6	1.1 to 6.1	0.029
Univariate models for the affected triceps brachii			
Fat percentage	-0.36	-0.60 to -0.12	0.004
Total CSA *	0.30	0.09 to 0.50	0.005
Contractile CSA #	0.33	0.10 to 0.55	0.005

*The CSA including muscle tissue and intramuscular fat tissue, #contractile CSA = total CSA (100 - mean fat percentage) / 100. Univariate logistic regression models evaluated the contribution of fat percentage, total CSA or contractile CSA of the affected biceps or triceps brachii to the muscle force in MRC 0 to 3 versus MRC 4 and 5. The multivariate models were used to correct for age and time after trauma. Multivariate models of the affected triceps brachii are not shown because of invalid model due zero frequencies. MRC: medical research council, CI: confidence interval, CSA: cross sectional area.

Table VII: Linear regression for muscle force in Newton

Outcome variable	Regression coefficient	95% CI	*p* - value
Univariate models for the affected biceps brachii*			
Fat percentage	-10.3	-15.8 to -4.9	0.001
Total CSA *	12.3	8.5 to 16.1	< 0.001
Contractile CSA #	13.0	9.2 to 16.8	< 0.001
Multivariate models for the affected biceps brachii*			
Fat percentage	-10.3	-16.4 to 4.2	0.003
Total CSA *	12.2	8.1 to 16.3	< 0.001
Contractile CSA #	13.0	8.9 to 17.1	< 0.001
Univariate models for the affected triceps brachii*			
Fat percentage	-15.0	-23.2 to -6.7	0.001
Total CSA *	11.1	6.4 to 15.7	< 0.001
Contractile CSA #	11.7	6.9 to 16.4	< 0.001

Table VII: Linear regression for muscle force in Newton (*continued*)

Outcome variable	Regression coefficient	95% CI	*p* - value
Multivariate models for the affected triceps brachii*			
Fat percentage	-15.4	-24.4 to -6.4	0.002
Total CSA *	12.6	8.3 to 16.9	< 0.001
Contractile CSA #	13.2	8.8 to 17.6	< 0.001
Univariate models for the non-affected biceps brachii			
Fat percentage	-13.4	-41.0 to 14.3	0.323
Total CSA *	7.4	3.6 to 11.2	0.001
Contractile CSA #	7.8	3.8 to 11.8	0.001
Multivariate models for the non-affected biceps brachii			
Fat percentage	-11.9	-40.9 to 17.1	0.396
Total CSA *	7.5	3.5 to 11.5	0.001
Contractile CSA #	7.9	3.6 to 12.1	0.001
Univariate models for the non-affected triceps brachii			
Fat percentage	-1.2	-21.9 to 19.4	0.902
Total CSA *	6.0	-1.0 to 13.0	0.086
Contractile CSA #	6.4	-1.0 to 13.8	0.087
Multivariate models for the non-affected triceps brachii			
Fat percentage	-11.6	-32.2 to 8.9	0.245
Total CSA *	4.1	-3.6 to 11.7	0.270
Contractile CSA #	4.4	-3.4 to 12.3	0.247

*The CSA including muscle tissue and intramuscular fat tissue, #contractile CSA = total CSA (100 - mean fat percentage) / 100. Univariate linear regression models evaluated the contribution of fat percentage, total CSA or contractile CSA of the affected or non-affected biceps or triceps brachii to the muscle force in Newton. *Only n=12 patients were included in these regression models because these patients were able to give muscle force against resistance, i.e. Muscle Research Council (MRC) 4 or 5. The multivariate models were used to correct for age and time after trauma. CI: confidence interval, CSA: cross sectional area.

DISCUSSION

The three-point Dixon MRI quantifies intramuscular fat, total and contractile CSA with an excellent inter-observer reliability in BPI patients. The fat percentage, total and contractile CSA was shown to be homogenous among consecutive MRI slices. The fat percentage of both the biceps and the triceps brachii showed a strong association with the Goutallier score, but the Goutallier score overestimated the fat percentage compared to the Dixon technique. Contractile CSA of the affected biceps brachii contributed most to the reduction in active elbow flexion, active supination and muscle force.

Long-term denervation results in muscle degeneration including muscle atrophy and fatty degeneration. Previous studies in brachial plexus injury used only qualitative methods to score muscular fatty degeneration [4, 9]. Contrary, with quantitative measurement methods comparisons between but also within patient groups during follow-up are more objective. Quantitative MRI has previously been used in patients with rotator cuff tears, in aging and Duchene muscular dystrophy. The values of control patients in literature are comparable with our observation of fat percentage of 6 ± 1.0 % in the non-affected biceps brachii [28, 34]. As hypothetically expected, but never been proved in a clinical setting, contractile CSA was also associated with muscle force of the non-affected biceps brachii indicating a consistent measurement method. Using both quantitative MRI and quantitative muscle force, we calculated the specific muscle force. This excluded the non-functional fat inside the muscle compartment. The specific muscle force was significantly lower in the affected compared to the non-affected biceps brachii, indicating a lower muscle quality in the affected muscle. In BPI, the limited capacity of muscle fibers to contract could be due to the partial denervation, but also muscle stiffness or disorganization of the muscle fibers could influence the capacity of the muscle fibers to generate force [35, 36].

The quantitative three-point Dixon method showed a good correlation with the qualitative T1 measurements of fat using the Goutallier score. As previously described, the Goutallier score gave an overestimation of the intramuscular fat [19]. Other quantitative techniques used to assess fatty degeneration in BPI include ultrasound and computed tomography. However these techniques result in a value for muscle attenuation without the possibility to distinguish between muscle and fat tissue [13, 37]. This is the first study using a quantitative assessment of contractile CSA in BPI patients. Five consecutive MRI slices showed a homogeneous distribution of intramuscular fat, total and contractile CSA. It is not known whether this distribution is also homogeneous along the total length of the muscles as the proximal and distal end of the muscles were not included in the MRI scans in this study.

Strength of this study is the use of the non-affected arm as a control and the association of quantitative MRI data with clinical parameters as range of motion and muscle force. A limitation of this study is a lack of histology; however literature shows an excellent correlation of fat fraction obtained by MRI and histology [38].

Measurements of fat percentage, total and contractile CSA may give more insight into the pathophysiology of contractures and muscle weakness in traumatic BPI as well as neonatal BPI. It could be used to predict which patients are more likely to progress to a worse outcome due to bony deformities and assist at the timing of surgery. Dixon MRI may also improve treatment of BPI by determining which patients favor which type of surgery including contracture releases, tendon

transfers and osteotomies. Measurement of contractile CSA may be used to assess the muscle imbalance around the shoulder in neonatal brachial plexus palsy which causes glenohumeral deformities [4, 10, 12]. Knowledge on this muscle imbalance could assist at decision making on the timing and what kind of operation to perform to prevent glenohumeral deformities. Furthermore, quantitative assessment of fat percentage, total and contractile CSA might be useful in longitudinal follow-up and for research purposes [13]. The contractile CSA of the affected biceps brachii contributed most to the reduction in active flexion, active supination and muscle force. The fat percentage also contributed to clinical outcome, although this contribution was less strong compared to atrophy. As contractile CSA contributed most to clinical outcome, we favor measurement of both the fat percentage and the total CSA to be able to calculate the contractile CSA. Contractile CSA may be the best parameter to quantify muscle atrophy and fatty degeneration, however this will need to be confirmed in future research.

CONCLUSIONS

This study showed that the intramuscular fat, the total and contractile CSA of the biceps and triceps brachii can be assessed in BPI with an excellent reliability. The quantitative scoring of the three-point Dixon sequences was significantly correlated with the qualitative Goutallier score on T1 weighted TSE sequences, however the Goutallier score gave an overestimation. The contractile CSA of the affected biceps contributed most to the reduction in active flexion, active supination and muscle force. Assessment of contractile CSA will yield valuable insight in pathophysiology and predict the outcome of conservative and surgical procedures.

ACKNOWLEDGEMENTS

This study was funded by the Dutch Arthritis Association (LLR13) and the Program Translational Research of ZonMw, the Netherlands organization for health research and development (project number 95100105), which did not play a role in the investigation. We would like to thank Beatrijs H.A. Wokke for assistance at MRI acquisition and we would like to thank Carla S.P. van Rijswijk for qualitative MRI scoring.

REFERENCES

1. Kim DH, Cho YJ, Tiel RL, Kline DG. Outcomes of surgery in 1019 brachial plexus lesions treated at Louisiana State University Health Sciences Center. J Neurosurg 2003; 98:1005-1016.
2. Malessy MJ, de Ruiter GC, de Boer KS, Thomeer RT. Evaluation of suprascapular nerve neurotization after nerve graft or transfer in the treatment of brachial plexus traction lesions. J Neurosurg 2004; 101:377-389.
3. Krishnan KG, Martin KD, Schackert G. Traumatic lesions of the brachial plexus: an analysis of outcomes in primary brachial plexus reconstruction and secondary functional arm reanimation. Neurosurgery 2008; 62:873-885.
4. Hogendoorn S, van Overvest KL, Watt I, Duijsens AH, Nelissen RG. Structural changes in muscle and glenohumeral joint deformity in neonatal brachial plexus palsy. J Bone Joint Surg Am 2010; 92:935-942.
5. Hale HB, Bae DS, Waters PM. Current concepts in the management of brachial plexus birth palsy. J Hand Surg Am 2010; 35:322-331.
6. Malessy MJ, Pondaag W. Neonatal brachial plexus palsy with neurotmesis of C5 and avulsion of C6: supraclavicular reconstruction strategies and outcome. J Bone Joint Surg Am 2014; 96:e174.
7. Eismann EA, Little KJ, Laor T, Cornwall R. Glenohumeral abduction contracture in children with unresolved neonatal brachial plexus palsy. J Bone Joint Surg Am 2015; 97:112-118.
8. Poyhia TH, Nietosvaara YA, Remes VM, Kirjavainen MO, Peltonen JI, Lamminen AE. MRI of rotator cuff muscle atrophy in relation to glenohumeral joint incongruence in brachial plexus birth injury. Pediatr Radiol 2005; 35:402-409.
9. Poyhia TH, Koivikko MP, Peltonen JI, Kirjavainen MO, Lamminen AE, Nietosvaara AY. Muscle changes in brachial plexus birth injury with elbow flexion contracture: an MRI study. Pediatr Radiol 2007; 37:173-179.
10. Waters PM, Monica JT, Earp BE, Zurakowski D, Bae DS. Correlation of radiographic muscle cross-sectional area with glenohumeral deformity in children with brachial plexus birth palsy. J Bone Joint Surg Am 2009; 91:2367-2375.
11. VAN Gelein Vitringa VM, Jaspers R, Mullender M, Ouwerkerk WJ, van der Sluijs JA. Early effects of muscle atrophy on shoulder joint development in infants with unilateral birth brachial plexus injury. Dev Med Child Neurol 2010.
12. Ruoff JM, van der Sluijs JA, van Ouwerkerk WJ, Jaspers RT. Musculoskeletal growth in the upper arm in infants after obstetric brachial plexus lesions and its relation with residual muscle function. Dev Med Child Neurol 2012; 54:1050-1056.
13. Hogendoorn S, Duijnisveld BJ, van Duinen SG, Stoel BC, van Dijk JG, Fibbe WE, Nelissen RG. Local injection of autologous bone marrow cells to regenerate muscle in patients with traumatic brachial plexus injury: a pilot study. Bone Joint Res 2014; 3:38-47.
14. Slabaugh MA, Friel NA, Karas V, Romeo AA, Verma NN, Cole BJ. Interobserver and intraobserver reliability of the Goutallier classification using magnetic resonance imaging: proposal of a simplified classification system to increase reliability. Am J Sports Med 2012; 40:1728-1734.
15. Jain NB, Collins J, Newman JS, Katz JN, Losina E, Higgins LD. Reliability of Magnetic Resonance Imaging Assessment of Rotator Cuff: The ROW Study. PM R 2015; 7:245-254.
16. Fischmann A, Hafner P, Fasler S, Gloor M, Bieri O, Studler U, Fischer D. Quantitative MRI can detect subclinical disease progression in muscular dystrophy. J Neurol 2012; 259:1648-1654.

17. Willis TA, Hollingsworth KG, Coombs A, Sveen ML, Andersen S, Stojkovic T, Eagle M, Mayhew A, de Sousa PL, Dewar L, Morrow JM, Sinclair CD, Thornton JS, Bushby K, Lochmuller H, Hanna MG, Hogrel JY, Carlier PG, Vissing J, Straub V. Quantitative muscle MRI as an assessment tool for monitoring disease progression in LGMD2I: a multicentre longitudinal study. PLoS One 2013; 8:e70993.
18. Willis TA, Hollingsworth KG, Coombs A, Sveen ML, Andersen S, Stojkovic T, Eagle M, Mayhew A, de Sousa PL, Dewar L, Morrow JM, Sinclair CD, Thornton JS, Bushby K, Lochmuller H, Hanna MG, Hogrel JY, Carlier PG, Vissing J, Straub V. Quantitative magnetic resonance imaging in limb-girdle muscular dystrophy 2I: a multinational cross-sectional study. PLoS One 2014; 9:e90377.
19. Nardo L, Karampinos DC, Lansdown DA, Carballido-Gamio J, Lee S, Maroldi R, Ma CB, Link TM, Krug R. Quantitative assessment of fat infiltration in the rotator cuff muscles using water-fat MRI. J Magn Reson Imaging 2014; 39:1178-1185.
20. Lee S, Lucas RM, Lansdown DA, Nardo L, Lai A, Link TM, Krug R, Ma CB. Magnetic resonance rotator cuff fat fraction and its relationship with tendon tear severity and subject characteristics. J Shoulder Elbow Surg 2015.
21. Kovanlikaya A, Mittelman SD, Ward A, Geffner ME, Dorey F, Gilsanz V. Obesity and fat quantification in lean tissues using three-point Dixon MR imaging. Pediatr Radiol 2005; 35:601-607.
22. Karampinos DC, Baum T, Nardo L, Alizai H, Yu H, Carballido-Gamio J, Yap SP, Shimakawa A, Link TM, Majumdar S. Characterization of the regional distribution of skeletal muscle adipose tissue in type 2 diabetes using chemical shift-based water/fat separation. J Magn Reson Imaging 2012; 35:899-907.
23. Alizai H, Nardo L, Karampinos DC, Joseph GB, Yap SP, Baum T, Krug R, Majumdar S, Link TM. Comparison of clinical semi-quantitative assessment of muscle fat infiltration with quantitative assessment using chemical shift-based water/fat separation in MR studies of the calf of post-menopausal women. Eur Radiol 2012; 22:1592-1600.
24. Wren TA, Bluml S, Tseng-Ong L, Gilsanz V. Three-point technique of fat quantification of muscle tissue as a marker of disease progression in Duchenne muscular dystrophy: preliminary study. AJR Am J Roentgenol 2008; 190:W8-12.
25. Wokke BH, Bos C, Reijnierse M, van Rijswijk CS, Eggers H, Webb A, Verschuuren JJ, Kan HE. Comparison of dixon and T1-weighted MR methods to assess the degree of fat infiltration in duchenne muscular dystrophy patients. J Magn Reson Imaging 2013; 38:619-624.
26. van den Bergen JC, Wokke BH, Janson AA, van Duinen SG, Hulsker MA, Ginjaar HB, van Deutekom JC, Aartsma-Rus A, Kan HE, Verschuuren JJ. Dystrophin levels and clinical severity in Becker muscular dystrophy patients. J Neurol Neurosurg Psychiatry 2014; 85:747-753.
27. Triplett WT, Baligand C, Forbes SC, Willcocks RJ, Lott DJ, DeVos S, Pollaro J, Rooney WD, Sweeney HL, Bonnemann CG, Wang DJ, Vandenborne K, Walter GA. Chemical shift-based MRI to measure fat fractions in dystrophic skeletal muscle. Magn Reson Med 2014; 72:8-19.
28. Wokke BH, van den Bergen JC, Versluis MJ, Niks EH, Milles J, Webb AG, van Zwet EW, Aartsma-Rus A, Verschuuren JJ, Kan HE. Quantitative MRI and strength measurements in the assessment of muscle quality in Duchenne muscular dystrophy. Neuromuscul Disord 2014; 24:409-416.
29. Carlier PG, Azzabou N, de Sousa PL, Hicks A, Boisserie JM, Amadon A, Carlier RY, Wary C, Orlikowski D, Laforet P. Skeletal muscle quantitative nuclear magnetic resonance imaging follow-up of adult Pompe patients. J Inherit Metab Dis 2015; 38:565-572.

30. Wary C, Azzabou N, Giraudeau C, Le LJ, Montus M, Voit T, Servais L, Carlier P. Quantitative NMRI and NMRS identify augmented disease progression after loss of ambulation in forearms of boys with Duchenne muscular dystrophy. NMR Biomed 2015.
31. Narakas AO. Obstetrical brachial plexus injuries. In: Lamb D, editor. The paralysed hand. Edinburgh: 1987. p 116-135.
32. Shrout PE, Fleiss JL. Intraclass correlations: uses in assessing rater reliability. Psychol Bull 1979; 86:420-428.
33. Cicchetti DV, Sparrow SA. Developing criteria for establishing interrater reliability of specific items: applications to assessment of adaptive behavior. Am J Ment Defic 1981; 86:127-137.
34. Hogrel JY, Barnouin Y, Azzabou N, Butler-Browne G, Voit T, Moraux A, Leroux G, Behin A, McPhee JS, Carlier PG. NMR imaging estimates of muscle volume and intramuscular fat infiltration in the thigh: variations with muscle, gender, and age. Age (Dordr) 2015; 37:9798.
35. Galban CJ, Maderwald S, Uffmann K, de GA, Ladd ME. Diffusive sensitivity to muscle architecture: a magnetic resonance diffusion tensor imaging study of the human calf. Eur J Appl Physiol 2004; 93:253-262.
36. Chan S, Head SI, Morley JW. Branched fibers in dystrophic mdx muscle are associated with a loss of force following lengthening contractions. Am J Physiol Cell Physiol 2007; 293:C985-C992.
37. van de Sande MA, Stoel BC, Obermann WR, Lieng JG, Rozing PM. Quantitative assessment of fatty degeneration in rotator cuff muscles determined with computed tomography. Invest Radiol 2005; 40:313-319.
38. Gaeta M, Scribano E, Mileto A, Mazziotti S, Rodolico C, Toscano A, Settineri N, Ascenti G, Blandino A. Muscle fat fraction in neuromuscular disorders: dual-echo dual-flip-angle spoiled gradient-recalled MR imaging technique for quantification--a feasibility study. Radiology 2011; 259:487-494.